

Binding Mechanism and Synergetic Effects of Xanthone Derivatives as Noncompetitive α -Glucosidase Inhibitors: A Theoretical and Experimental Study

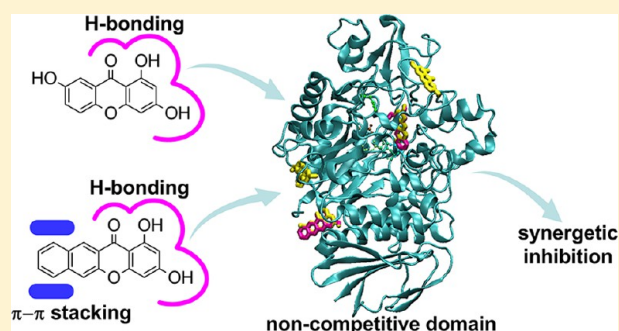
Yan Liu,[†] Lin Ma,[†] Wen-Hua Chen,^{*,‡} Hwangseo Park,[§] Zhuofeng Ke,^{*,†} and Bo Wang^{*,†}

[†]MOE Key Laboratory of Bioinorganic and Synthetic Chemistry/KLGHEI of Environment and Energy Chemistry, School of Chemistry & Chemical Engineering, Sun Yat-sen University, Guangzhou 510275, PR China

[‡]School of Pharmaceutical Sciences, Southern Medical University, Guangzhou 510515, PR China

[§]Department of Bioscience and Biotechnology, Sejong University, 98 Kunja-Dong, Kwangjin-Ku, Seoul 143-747, Korea

ABSTRACT: Newly emerged xanthone derivatives have attracted considerable interests as a novel class of potent α -glucosidase inhibitors. To provide insights into the inhibitory and binding mechanisms of xanthone-based inhibitors toward α -glucosidase, we carried out experimental and theoretical studies on two typical xanthone derivatives, i.e., 1,3,7-trihydroxyxanthone and 1,3-dihydroxybenzoxanthone. The results indicate that these two xanthone derivatives belong to noncompetitive inhibitors and induce a loss in the α -helix content of the secondary structure of α -glucosidase. Docking simulation revealed the existence of multiple binding modes, in which polyhydroxyl groups and expanded aromatic rings acted as two key pharmacophores to form H-bonding and π - π stacking interactions with α -glucosidase. The fact that 1,3,7-trihydroxyxanthone and 1,3-dihydroxybenzoxanthone exhibited significant synergetic inhibition to α -glucosidase strongly suggests that both xanthone derivatives simultaneously bind to the distinct noncompetitive sites of yeast's α -glucosidase. On the basis of the plausible binding clues, synergetic inhibition can be developed to be a promising strategy to achieve enhanced inhibitory activities.



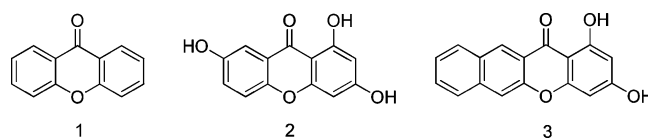
1. INTRODUCTION

α -Glucosidase (EC 3.2.1.20) plays a key role in the digesting of carbohydrates as well as in the processing of glycoproteins and glycolipids, which are closely related to some modern diseases, such as diabetes, HIV, and cancers.^{1–8} Inhibition of α -glucosidase in the digestive tract can prevent carbohydrate digestion and impact the carbohydrate digestion time. Thus, α -glucosidase inhibitors may be used as attractive therapeutic agents to reduce the rate of glucose absorption and consequently suppress the levels of postprandial blood glucose and insulin.^{7–10} It is also reported that α -glucosidase inhibitors can alter glycosylation and reduce the total amount of some glycoproteins produced.^{7,11} Therefore, inhibiting the action of α -glucosidase may lead to the discovery of new therapeutic agents for these diseases. During the past few decades, considerable efforts have been devoted to the creation of α -glucosidase inhibitors,^{7,12–16} which can be classified into sugar-mimicking and non-sugar types according to their structural features.^{17–19} To date, sugar-mimicking α -glucosidase inhibitors have been extensively studied, and some of them, including acarbose (Bayer), miglitol (Bayer), and voglibose (Takeda), have been clinically used to inhibit small intestinal α -glucosidase hydrolases, such as α -glucosidase, glucoamylase (EC 3.2.1.3), and sucrase (EC 3.2.1.48).⁵ Though non-sugar α -glucosidase inhibitors are essential as therapeutic agents in

terms of diversity, they have not yet been well developed relative to sugar-containing inhibitors.

Toward this end, we have been keenly interested in xanthone (1, Chart 1) and its derivatives as alternate potent non-sugar

Chart 1. Structures of Xanthone and Typical Xanthone Derivatives



inhibitors.^{20–35} This is spurred by the fact that xanthones are natural components widely distributed in medicinal plants such as *Bonnetiaceae* and *Clusiaceae*, and exhibit multiple pharmacological biological activities, including antitumor,^{32,33} anti-inflammatory,³⁶ antithrombotic,³⁷ and eukaryote kinase effects.³⁸ Because xanthones are structurally different from sugar-mimicking inhibitors, they should, in principle, exert their inhibitory activities *via* a different mechanism of ac-

Received: July 8, 2013

Revised: September 30, 2013

tion.^{20–23,39,40} In previous studies, we have shown that polyhydroxylation and expanded π -conjugation of xanthenes, for example, to give compounds 2 and 3 (Chart 1), respectively, lead to a remarkable enhancement in the inhibitory activities, which was further verified by subsequent quantitative structure–activity relationships (QSAR) study.^{20–23} These studies have provided some valuable implications for the probable interactions of xanthone derivatives with α -glucosidase. However, their binding modes and the mechanism of action remain to be clarified. Specifically, the issues that are of particular interest to us include (1) the binding manners and inhibitory actions of xanthenes with α -glucosidase; (2) the detailed structural information of the binding site(s); (3) the interactions that play key roles in each binding mode; and (4) the possible guidelines for future structure-based drug design of xanthone-based inhibitors with potent activities.

To address these issues, we carried out experimental and computational investigations on two typical xanthone derivatives, i.e., compounds 2 and 3. Enzyme kinetics were measured by using Lineweaver–Burk plots. The probable binding modes, the specificity of the binding sites, and their topography were studied by means of docking simulation. Combined administrations of compounds 2 and 3 were further performed to examine the potentiality of synergetic effects as a practical strategy to enhance the inhibitory activities of xanthone derivatives.

2. EXPERIMENTAL AND THEORETICAL METHODS

2.1. Materials. *p*-Nitrophenyl (PNP) glycoside and α -glucosidase (from Baker's yeast) were purchased from Sigma (St. Louis, MO, USA). Compound 1 was purchased from Sigma-Aldrich (Sintra, Portugal). Compounds 2 and 3 were prepared according to reported protocols^{20–22} and fully characterized on the basis of NMR (¹H and ¹³C), mass, IR, and elemental analyses. All other reagents were of analytical grade and used as received.

2.2. Enzyme Assay. UV spectra were recorded on a Shimadzu UV-3150 scanning spectrophotometer. The inhibitory activities were measured by using the methods similar to those described previously.^{20–22} Typically, α -glucosidase activity was assayed in 50 mM phosphate buffer (pH 6.8) containing 5% v/v DMSO, and PNP glycoside was used as a substrate. Compounds 2 and 3 were preincubated with α -glucosidase at 37 °C for 30 min. After PNP glycoside was added, the enzymatic reaction was carried out at 37 °C for 60 s and monitored spectrophotometrically by measuring the absorbance at 400 nm. The assay was performed in triplicate with five different concentrations around the IC₅₀ values that were roughly estimated in the first round of experiments, and the mean values were adopted.

2.3. Kinetics of Enzyme Inhibition. The inhibition types of compounds 2 and 3 were determined from Lineweaver–Burk plots as previously described.^{41,42} Typically, two different concentrations of each compound around the IC₅₀ values were chosen. Under each concentration, α -glucosidase activity was assayed by varying the concentration of PNP glycoside. The enzymatic reaction was performed under the above-mentioned reaction condition. The mixtures of α -glucosidase with compounds 2 and 3 were dissolved in 50 mM phosphate buffer (pH 6.8) containing 5% v/v DMSO and preincubated at 37 °C for 30 min, and then, PNP glycoside was added. The enzymatic reaction was carried out at 37 °C for 60 s, and monitored spectrophotometrically by measuring the absorb-

ance at 400 nm. Inhibition types and K_i values of compounds 2 and 3 were determined by double-reciprocal plots.

2.4. Circular Dichroism (CD) Assay. The effects of compounds 2 and 3 on the secondary structure of α -glucosidase were examined with circular dichroism (CD) spectroscopy, using methods similar to those reported in the literature.^{43–45} CD spectra were acquired on a J-810 spectrometer (model J-810, Jasco Inc., Japan), using a parameter set of 1.0 nm bandwidth, 0.1 nm data pitch, 0.2 cm path length, and 1.0 s response time and a 200 nm/min scanning speed. All the measurements were performed in 50 mM phosphate buffer (pH 6.8). α -Glucosidase was preincubated first with compounds 2, 3, or their mixture, respectively, at a concentration of 10 or 20 μ M at 37 °C for 0.5 h. CD spectra (180–250 nm) of α -glucosidase treated with or without xanthenes were measured and corrected by subtraction of a blank corresponding to the solvent. The professional program JWSSE (JASCO) was used to estimate the secondary structure percentages of α -glucosidase, based on the method of Yang et al.⁴⁶

2.5. Homology Modeling of α -Glucosidase. Because structural information is not available for the eukaryotic α -glucosidase enzymes commonly used in biological assays, we carried out homology modeling of α -glucosidase from Baker's yeast with the procedure used by Park et al.^{47,48} This started with the retrieval of the amino acid sequence of α -glucosidase MAL12 from Baker's yeast that comprises 584 amino acid residues from the UniProt protein knowledgebase (<http://www.uniprot.org/>; accession number P53341). In order to find an appropriate structural template for homology modeling, we searched for the Protein Data Bank (PDB) at National Center for Biotechnology and Information (NCBI) using BLAST with the amino acid sequence of the target as input. The results showed that oligo-1,6-glucosidase from *Bacillus cereus* reveals the highest sequence identity (38.5%) with the target. Therefore, its X-ray crystal structure (PDB ID: 1UOK)⁴⁹ was selected as the template for homology modeling.

Sequence alignment between α -glucosidase from Baker's yeast and oligo-1,6-glucosidase from *Bacillus cereus* was then derived with the ClustalW package⁵⁰ using the BLOSUM matrices for scoring the alignments. On the basis of the best-scored sequence alignment, the structure of α -glucosidase from Baker's yeast was constructed using the MODELER 8v2 program.⁵¹ In this model building, we employed an optimization method involving conjugate gradients and molecular dynamics to minimize the violations of the spatial restraints. More specifically, the 3D structural model was obtained from the optimization of molecular probability density function. With respect to the structure of gap regions, the coordinates were built from a randomized and distorted structure that is located approximately between the two anchoring regions as implemented in MODELER 8v2. In selecting the final model of the target from the various 3-D structures generated in the homology modeling, we used the MODELER objective function because it measures the extent of violation from the spatial restraints. Then, we calculated the conformational energy of the predicted structure of α -glucosidase with the ProSa 2003 program⁵² for the purpose of a final evaluation.

2.6. Docking Simulations. AutoDock Tools were used to assign Gasteiger partial charges and merge non-polar hydrogen atoms. The rigid protein structure of α -glucosidase was used as a receptor for the docking calculations. To obtain the most

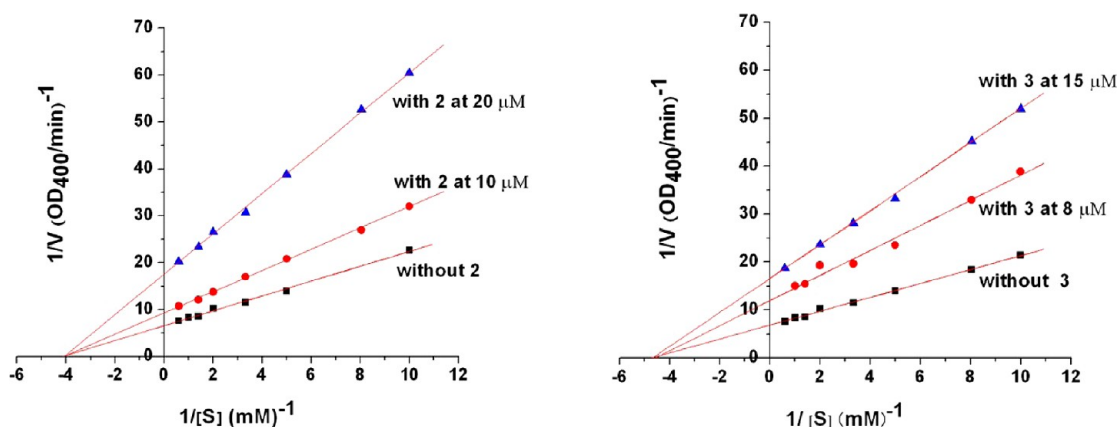


Figure 1. Double-reciprocal plots of the inhibition kinetics of yeast's α -glucosidase by compounds **2** and **3**. α -Glucosidase was incubated first with compounds **2** and **3** at 37 °C for 0.5 h, and then *p*-nitrophenyl (PNP) glycoside of varying concentrations was added to initiate the enzymatic reaction.

plausible binding sites, we searched the whole 3-D space of the receptors, including both the active-site and non-active-site regions. The grid maps were calculated in a grid box of $120 \times 120 \times 120$ points with a grid-point spacing of 0.640 Å. All the calculations were performed with the AutoDock4.2 program.⁵³ The docking simulations were performed with the Lamarckian genetic algorithm for at least 80 docking runs for each ligand, using a population size of 250 individuals with a maximum number of energy evaluations at 2.5×10^8 and a maximum number of generations at 2.7×10^4 . An extended model was used to estimate the energetics of the unbound states of the receptor and the ligands when evaluating their binding free energies (ΔG).⁵³ This binding free energy estimation mainly involves two steps: (a) the intramolecular energetics is estimated for the transition from unbound states to the conformation of the ligand and protein in the bound state; (b) evaluation of the intermolecular energetics of combining the ligand and protein in their bound conformation. Particularly, we employed an extended conformation of the ligand as the unbound state to calculate the ligand internal energy.

3. RESULTS AND DISCUSSION

3.1. Enzyme Kinetics. It is well-known that enzyme kinetics can provide some useful information about how a ligand interacts with its enzyme. To clarify how and where xanthenes bind to α -glucosidase, we first measured the enzyme kinetics of compounds **2** and **3** by using methods similar to those described in the literature.^{41,42} The obtained double-reciprocal plots are shown in Figure 1. It can be seen that the plots show straight lines with the same Michaelis–Menten constant K_m , suggesting that compounds **2** and **3** are typical noncompetitive α -glucosidase inhibitors. In another words, both compounds **2** and **3** bound to the noncompetitive domain of yeast's α -glucosidase rather than to the active site. The inhibitory constants (K_i 's) were 3.8 μ M for compound **2** (20.0 μ M) and 2.2 μ M for compound **3** (15.0 μ M), respectively.

3.2. Inhibition Mechanism. To gain further insight into the inhibitory mechanism of xanthenes toward yeast's α -glucosidase as well as into their impacts on the activity of the enzyme at the noncompetitive domain, we examined the effects of compounds **2** and **3** on the secondary structure of α -glucosidase by means of circular dichroism (CD) spectroscopy. The contents of the secondary structure motifs of α -

glucosidase, including α -helix, β -sheet, and β -turn, are listed in Table 1.

Table 1. The Effect of Compounds **2** and **3** and Their 3:7 Mixture on the Secondary Structure of Yeast's α -Glucosidase^a

inhibitor	conc. (μ M)	α -helix (%)	α -helix loss (%)	β -sheet (%)	β -turn (%)	random (%)
none		41.6		32.7	3.4	22.3
2	10	38.2	8.2	24.0	10.4	27.4
	20	33.1	20.4	33.3	5.2	28.4
3	10	35.1	15.6	29.6	7.8	27.4
	20	30.8	26.0	39.4	4.0	25.8
2 + 3	10	32.5	21.9	31.1	6.6	27.4
	20	24.8	40.4	44.2	4.6	26.4

^aMeasured in 50 mM phosphate buffer (pH 6.8) at 25 °C.

It can be seen from Table 1 that the content of α -helix within the secondary structure of α -glucosidase significantly decreased with the increase in the concentrations of compounds **2** and **3**. For example, in the presence of compounds **2** and **3** at a concentration of 20 μ M, the content of α -helix decreased from 41.6 to 33.1 and 30.8%, respectively, representing 20.4 and 26.0% loss of the α -helix in yeast's α -glucosidase, respectively. These results suggest that xanthone derivatives induce a loss of the α -helix within the secondary structure of α -glucosidase. It is known that α -helix is a relatively rigid secondary structure of protein and plays a crucial role in maintaining the conformation and exerting the catalytic function of an enzyme. Therefore, the loss of α -helix content may result in a change in the conformation of α -glucosidase, which may have a significant influence on the formation of an effective active site and subsequently on the enzyme activities.

3.3. Homology Modeling. The final structural model of α -glucosidase obtained from homology modeling was tested with the ProSa 2003 program by examining whether the interaction of each residue with the remainder of the protein is maintained favorable. This program calculates the knowledge-based mean fields to judge the quality of protein folds, and has been widely used to measure the stability of a protein conformation.⁵² Figure 2 shows the ProSa 2003 energy profile of the homology-modeled α -glucosidase in comparison to that of the X-ray structure of oligo-1,6-glucosidase. It should be noted that the

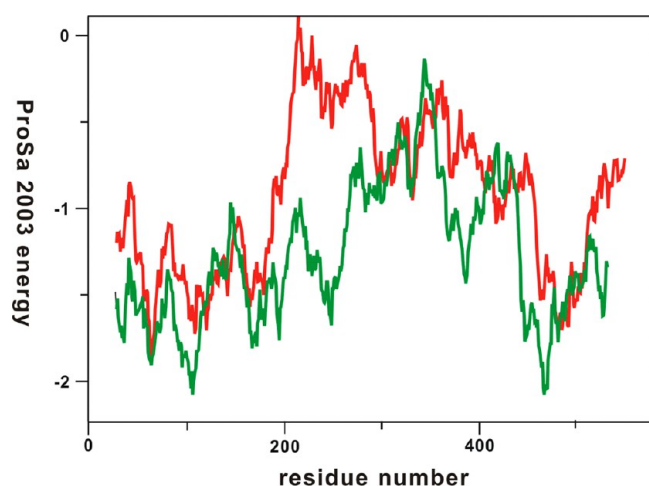


Figure 2. Comparison of the ProSa energy profiles for the homology-modeled structure of α -glucosidase (red) and the X-ray structure of oligo-1,6-glucosidase (green).

ProSa energy of α -glucosidase remains negative for all amino acid residues except for a few around a residue number of 210, indicating the acceptability of the homology modeled structure. This result supports the possibility that the homology modeling with a high sequence identity and a high-quality template structure can produce a 3-D structure of target protein comparable in accuracy to that determined from X-ray crystallography.⁵⁴

3.4. Binding Modes. Although both compounds 2 and 3 functioned in the noncompetitive domain of α -glucosidase and

induced a decline in the α -helix content, their binding modes appear different based on our previous observations that hydroxyl groups as H-bond donors and/or acceptors are important for polyhydroxyxanthenes, whereas an expanded conjugated aromatic ring is crucial to benzoxanthenes, implying the possible involvement of π - π stacking interactions.^{20–22} Therefore, it is of interest to explore the specificity and topography of their binding sites, and to elucidate the specific interactions that are responsible for the binding modes of different xanthone inhibitors.

To address these, we carried out docking simulations of compounds 2 and 3 with yeast's α -glucosidase protein model using the AutoDock4.2 program.⁵³ Although the three-dimensional structure of α -glucosidase is unavailable in the Protein Data Bank, the homology modeled structure proved to be useful, as it has been successfully applied in structure-based drug design.^{47,48,55} Therefore, we used the structure of Baker's yeast α -glucosidase, which was obtained from homology modeling using oligo-1,6-glucosidase from *Bacillus cereus*⁴⁹ as the structural template, in the docking simulations. The probable binding modes of compounds 2 and 3 with α -glucosidase, the associated binding free energies, and the key residues in the binding pockets are shown in Figures 3 and 4, respectively. The position of the active site of α -glucosidase is shown in Figure 5.

As shown in Figures 3 and 4, all the binding sites of compounds 2 and 3 are located at the noncompetitive domain of α -glucosidase, rather than at the active site. In other words, compounds 2 and 3 act as noncompetitive inhibitors, which is in full accordance with the aforementioned kinetic results (Figure 1). Binding modes 2A, 2B, 2C, and 3B are located away

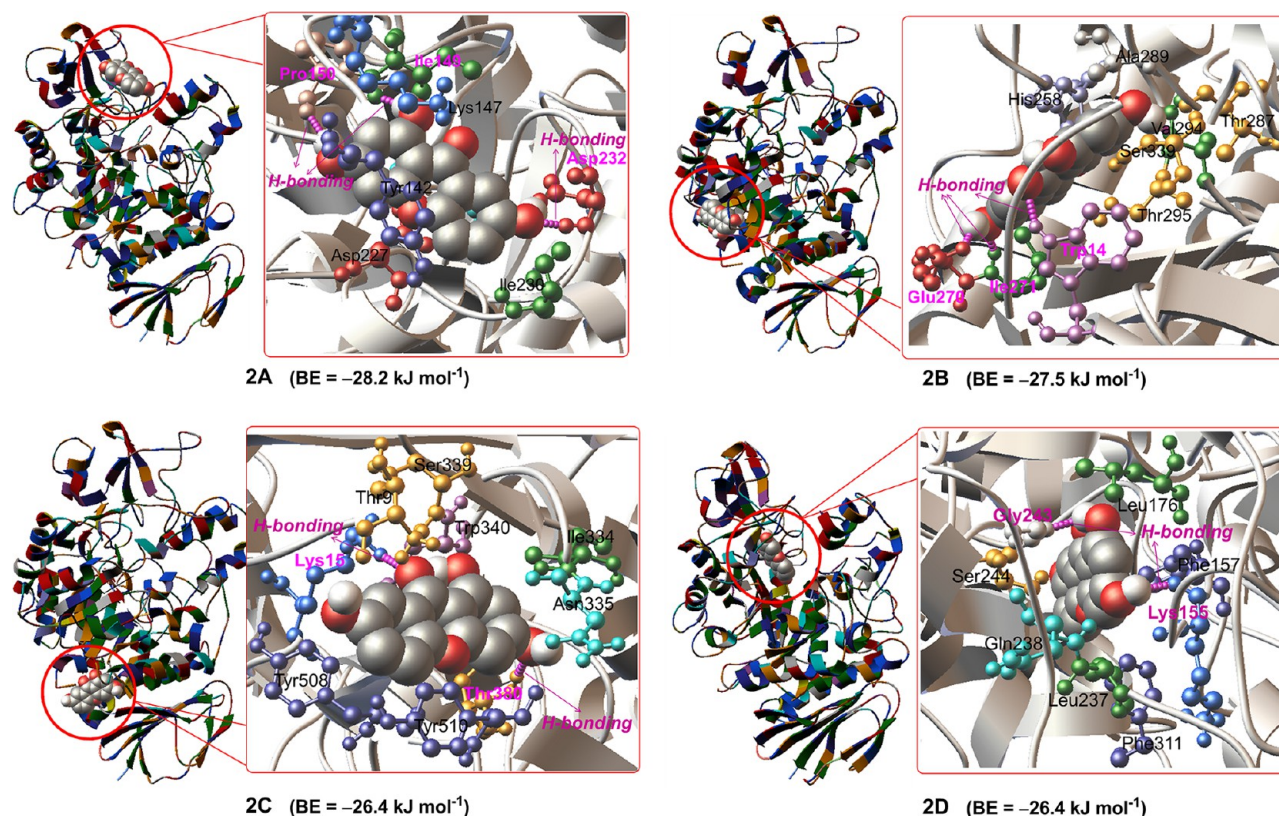


Figure 3. Four probable binding modes of compound 2 with α -glucosidase. Compound 2, the key residues, and the significant H-bonding interactions are shown in space-filling CPK display, stick-ball display, and purple dot lines, respectively. BE denotes the binding free energies.

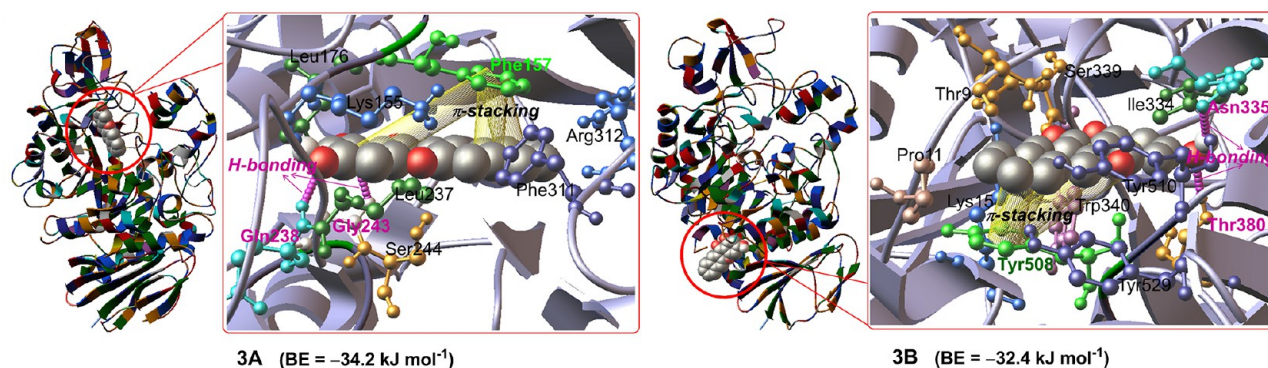


Figure 4. Two probable binding modes of compound 3 with α -glucosidase. Compound 3, the key residues, the significant H-bonding, and the π - π stacking interactions are shown in space-filling CPK display, stick-ball display, purple dot lines, and yellow column, respectively. BE denotes the binding free energies.

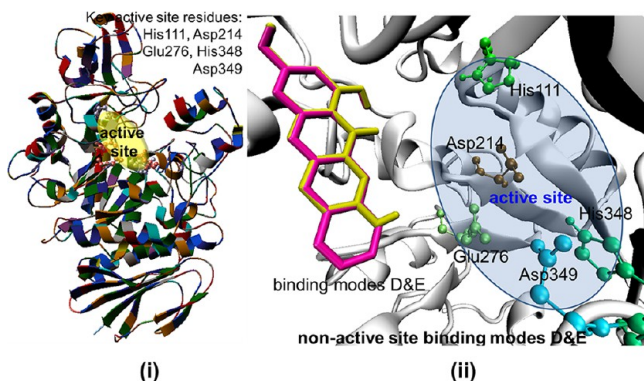


Figure 5. Nonactive site binding modes (2D in Figure 3 and 3A in Figure 4) in α -glucosidase. (i) The active site of α -glucosidase. (ii) The relative position of binding sites 2D and 3A, and the active site. Compounds 2 and 3 are highlighted in yellow and red, respectively.

from the active site, whereas binding modes 2D and 3A are relatively close to the active site. The binding site positions for modes 2D and 3A, the relative position of the active site, and the key residues are depicted in Figure 5. His111, Asp214, Glu276, Asp343, and His348 are key residues in the active site of α -glucosidase.^{47–49} It is clear that these residues are not involved in the binding modes 2D and 3A, suggesting that either compound 2 or 3 would be unlikely to compete with the substrate, *p*-nitrophenyl (PNP) glycoside, to bind to the active site.

It is noteworthy that compounds 2 and 3 have different binding characteristics, as shown in their suggested binding modes. Because compound 2 is a relatively small molecule, it has several probable binding modes, including 2A, 2B, 2C, and 2D (Figure 3). These binding modes have very similar binding free energies, ranging from -28.2 to -26.4 kJ mol⁻¹. Of the four binding modes, 2A is predicted to have the highest binding affinity. Interestingly, significant H-bonding interactions with the hydroxyl groups of compound 2 were found in all of these binding sites. In binding mode 2A, for example, the hydroxyl groups of compound 2 form H-bonds with the key residues Ile149, Pro150, and Asp232. Similar H-bonding interactions can be found with Trp14, Glu270, and Ile271 in binding mode 2B, with Lys15 and Thr380 in mode 2C, and with Lys155 and Gly243 in mode 2D. These results indicate that H-bonding interaction plays a key role in the binding modes of polyhydroxyxanthone derivatives, such as compound 2. This well accounts for the previous observation that polyhydroxyl

groups were essential to improve the inhibitory activity of xanthone 1.²¹

On the contrary, in addition to the H-bonding interactions, significant π - π stacking interaction was found in the binding modes of compound 3. As shown in Figure 4, docking simulations revealed the existence of two probable binding modes, 3A and 3B, with the estimated binding free energies being -34.2 and -32.4 kJ mol⁻¹, respectively. These binding pockets are located in the same positions as those in binding modes 2D and 2C, respectively. However, the binding free energies become more favorable when compound 2 is replaced with compound 3, due to the involvement of additional π - π stacking interactions. This finding is in good agreement with our previous observation that the presence of an extended π system made benzoxanthones more potent α -glucosidase inhibitors. In binding mode 3A, significant π - π stacking interaction was found between the conjugated skeleton of compound 3 and the side chain phenyl group of Phe157. In addition to this π - π stacking interaction, H-bonding interactions were also found with Gln238 and Gly342. In binding mode 3B, the π - π stacking interaction of the extended benzo-ring with Tyr508 and the H-bonding interaction with Asn335 and Thr380 were observed (Figure 4). These binding modes support our previous experimental implication that π - π stacking interaction might be the origin of the enhanced inhibitory activities shown by benzoxanthone derivatives.²⁰

The aforementioned results suggest that polyhydroxyl groups and extended aromatic rings can be regarded as two key pharmacophores for xanthone-based α -glucosidase inhibitors. These findings may provide some useful guidance for future drug design. It should be noted that several aromatic side chains, including Phe157 and Phe311 in binding mode 3A and Tyr508, Tyr510, and Tyr529 in binding mode 3B, are in proximity with compound 3, and could form additional π - π stacking interactions. In addition, some hydrophilic side chains of such residues as Lys, Arg, and Thr may form additional H-bonding interactions. Thus, more active xanthone inhibitors may be created by modulating the numbers and the topologies of polyhydroxyl groups and/or further expanding the aromatic rings. It is anticipated that the strong binding interaction of xanthones to the allosteric sites of α -glucosidase would probably perturb the protein structure, which may lead to a loss in the α helix content of the secondary structure of α -glucosidase during inhibition, as suggested by CD spectroscopy results.

3.5. Synergetic Inhibition. As shown above, all the proposed binding modes for compounds **2** and **3** have similar binding free energies, and thus none of them can be totally excluded. The fact that compounds **2** and **3** show obviously different binding manners implies that multiple binding sites may exist for xanthone inhibitors in the noncompetitive domain. Thus, one immediate concern we have is whether polyhydroxyxanthenes and benzoxanthenes are able to simultaneously bind to α -glucosidase, and cooperatively inhibit the action of α -glucosidase.

To clarify this, we investigated the inhibitory effect of compounds **2**, **3**, and their mixture in varying molar ratios, according to the reported assay method.^{41,56} As shown in Figure 6, compounds **2** (2 μ M) and **3** (2 μ M) inhibited the

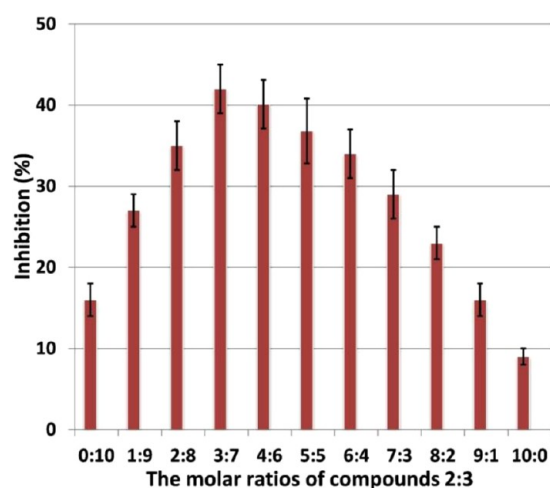


Figure 6. Inhibitory activities of compounds **2** (2 μ M), **3** (2 μ M), and their mixture (2 μ M) in varying molar ratios toward yeast's α -glucosidase. Each activity was measured in triplicate and repeated at least three times.

enzyme by 9.9 and 16.1%, respectively. However, their 1: 1 mixture (totally 2 μ M) inhibited the enzyme by 36.8%, which is 4- and 2-fold greater than those exhibited by compounds **2** and **3**, respectively. This result suggests that the combined administration of compounds **2** and **3** produced synergistic inhibition. It was reported that competitive inhibitors and noncompetitive inhibitors of α -glucosidase could produce a synergetic effect to enhance their inhibition.^{41,42} Our present observations provide an example that synergetic inhibition also exists among noncompetitive inhibitors.

Inspired by these observations, we are interested in determining the optimal ratio of compound **2** to compound **3** for their synergetic effect. Thus, a series of mixtures of compounds **2** and **3** with fixed total concentrations (2 μ M) but varying molar ratios was prepared and subject to enzymatic experiment. As shown in Figure 6, the optimal molar ratio of compound **2** to compound **3** was found to be 3:7. We consequently performed dose–response experiments to determine the IC_{50} values of the combined administration at this optimal ratio. 1-Deoxynojirimycin was adopted as a positive control. The results are summarized in Table 2. The obtained IC_{50} value of combination was 5.1 μ M, 3- and 2-fold higher than those of compound **2** (IC_{50} = 14.7 μ M) and compound **3** (IC_{50} = 9.3 μ M), respectively. These observations highlight the intriguing potential of xanthone-combined administration as a promising strategy to enhance their inhibitory potential.

Table 2. The Inhibitory Activities of Compounds **2** and **3** and Their 3:7 Mixture^a

compound	2	3	2 + 3
IC_{50} (μ M)	14.7 \pm 1.1	9.3 \pm 0.4	5.1 \pm 0.4

^aDetermined against yeast's α -glucosidase in 50 mM phosphate buffer (pH 6.8) containing 5% v/v DMSO at 37 $^{\circ}$ C. The experiments were performed in triplicate and repeated at least three times, and the mean values were adopted. 1-Deoxynojirimycin was adopted as a positive control and had an IC_{50} value of 26.4 μ M.

To further clarify the synergetic manner of compounds **2** and **3** in the inhibitory activity, the effect of their combination on the secondary structure of α -glucosidase was examined with CD assay. Using the similar approach aforementioned, the mixture of compounds **2** and **3** in the molar ratio of 3:7 was incubated with the enzyme. As shown in Table 1, the combination (totally 20 μ M) caused 40.4% loss of the α -helix in α -glucosidase, suggesting that the combination synergetically affected the secondary structure of α -glucosidase, resulting in an enhancement in the inhibition of α -glucosidase.

4. CONCLUSION

In summary, we have carried out experimental and docking simulation studies on two typical xanthone derivatives, 1,3,7-trihydroxyxanthone and 1,3-dihydroxybenzoxanthone, aiming at revealing the binding mechanism and providing guidance for future rational design of potent xanthone-based α -glucosidase inhibitors. Our results indicate that 1,3,7-trihydroxyxanthone and 1,3-dihydroxybenzoxanthone belong to noncompetitive inhibitors, and induce a loss of α -helix within the secondary structure of α -glucosidase, which may play a key role in the inhibitory process.

Docking simulations using the homology model of Baker's yeast α -glucosidase have provided insights into the binding mechanism at the molecular level. Specifically, several probable binding modes for 1,3,7-trihydroxyxanthone and 1,3-dihydroxybenzoxanthone were found to exist in the noncompetitive domain of α -glucosidase, in which H-bonding and π – π stacking are the most important binding interactions. 1,3,7-Trihydroxyxanthone and 1,3-dihydroxybenzoxanthone exhibit different binding interaction characteristics with α -glucosidase. The former has significant H-bonding interactions between polyhydroxyl groups and α -glucosidase, whereas the latter has both H-bonding and π – π stacking interactions of α -glucosidase with polyhydroxyl groups and the extended aromatic rings, respectively. Thus, polyhydroxyl groups and extended aromatic rings may be generalized as two key pharmacophores for xanthone inhibitors. Structural information from the suggested binding pockets implies that more potent xanthone inhibitors for α -glucosidase may be created, by modulating the numbers and the topologies of polyhydroxyl groups and/or aromatic rings.

Furthermore, 1,3,7-trihydroxyxanthone and 1,3-dihydroxybenzoxanthone exhibited synergetic inhibition toward yeast's α -glucosidase, suggesting that there may exist multiple binding sites in the noncompetitive domain of α -glucosidase. Both inhibitors may simultaneously bind to the noncompetitive domain to promote the synergistic inhibition of the enzyme activity. Thus, from a practical standpoint, combined administrations of xanthone derivatives may serve as a promising strategy to enhance the inhibitory activities. It can be envisioned that the synergetic inhibition between xanthenes

and other types of noncompetitive inhibitors, as well as with competitive inhibitors, may also be possible strategies for combined administrations, which is currently under active investigation in our laboratories.

AUTHOR INFORMATION

Corresponding Authors

*E-mail: whchen@smu.edu.cn (W.-H.C.).

*E-mail: kezhf3@mail.sysu.edu.cn (Z.K.).

*E-mail: ceswb@mail.sysu.edu.cn (B.W.).

Notes

The authors declare no competing financial interest.

ACKNOWLEDGMENTS

This work is supported by National Natural Science Foundation of China (Nos. 21272290 and 21203256), the "Hundred Talent Program" of Sun Yat-sen University, the Program for New Century Excellent Talents in University (NCET-11-0920), and the Department of Education of Guangdong Province, China. Facilities supported by the TH-1/GZ, Guangzhou Supercomputing Center, the high-performance grid computing platform of Sun Yat-sen University, the Guangdong Province Key Laboratory of Computational Science, and the Guangdong Province Computational Science Innovative Research Team are also acknowledged.

REFERENCES

- (1) Truscheit, E.; Frommer, W.; Junge, B.; Muller, L.; Schmidt, D. D.; Wingender, W. Chemistry and Biochemistry of Microbial Alpha-Glucosidase Inhibitors. *Angew. Chem., Int. Ed. Engl.* **1981**, *20*, 744–761.
- (2) McCulloch, D. K.; Kurtz, A. B.; Tattersall, R. B. A New Approach to the Treatment of Nocturnal Hypoglycemia Using Alpha-Glucosidase Inhibition. *Diabetes Care* **1983**, *6*, 483–487.
- (3) Lee, D.-S.; Lee, S.-H. Genistein, a soy isoflavone, is a potent α -glucosidase inhibitor. *FEBS Lett.* **2001**, *501*, 84–86.
- (4) Sou, S.; Takahashi, H.; Yamasaki, R.; Kagechika, H.; Endo, Y.; Hashimoto, Y. α -Glucosidase Inhibitors with a 4, 5, 6, 7-Tetrachlorophthalimide Skeleton Pendanted with a Cycloalkyl or Dicarba-closo-dodecaborane Group. *Chem. Pharm. Bull.* **2001**, *49*, 791–793.
- (5) Hakamata, W.; Kurihara, M.; Okuda, H.; Nishio, T.; Oku, T. Design and Screening Strategies for α -Glucosidase Inhibitors Based on Enzymological Information. *Curr. Top. Med. Chem.* **2009**, *9*, 3–12.
- (6) de Melo, E. B.; Gomes, A. D.; Carvalho, I. α - and β -Glucosidase inhibitors: chemical structure and biological activity. *Tetrahedron* **2006**, *62*, 10277–10302.
- (7) Kajimoto, T.; Node, M. Inhibitors Against Glycosidases as Medicines. *Curr. Top. Med. Chem.* **2009**, *9*, 13–33.
- (8) Tundis, R.; Loizzo, M. R.; Menichini, F. Natural Products as α -Amylase and α -Glucosidase Inhibitors and their Hypoglycaemic Potential in the Treatment of Diabetes: An Update. *Mini-Rev. Med. Chem.* **2010**, *10*, 315–331.
- (9) Ross, S. A.; Gulve, E. A.; Wang, M. H. Chemistry and biochemistry of type 2 diabetes. *Chem. Rev.* **2004**, *104*, 1255–1282.
- (10) Chiasson, J. L.; Rabasa-Lhoret, M. Prevention of type 2 diabetes - Insulin resistance and beta-cell function. *Diabetes* **2004**, *53*, S34–S38.
- (11) Robina, I.; Moreno-Vargas, A. J.; Carmona, A. T.; Vogel, P. Glycosidase inhibitors as potential HIV entry inhibitors? *Curr. Drug Metab.* **2004**, *5*, 329–361.
- (12) Wardrop, D. J.; Waidyarachchi, S. L. Synthesis and biological activity of naturally occurring α -glucosidase inhibitors. *Nat. Prod. Rep.* **2010**, *27*, 1431–1468.
- (13) Gao, H.; Kawabata, J. α -glucosidase inhibition of 6-hydroxyflavones. Part 3: Synthesis and evaluation of 2,3,4-trihydroxybenzoyl-containing flavonoid analogs and 6-aminoflavones as α -glucosidase inhibitors. *Bioorg. Med. Chem.* **2005**, *13*, 1661–1671.
- (14) Asano, N.; Kizu, H.; Oseki, K.; Tomioka, E.; Matsui, K. N-Alkylated Nitrogen-in-the-Ring Sugars: Conformational Basis of Inhibition of Glycosidases and HIV-1 Replication. *J. Med. Chem.* **1995**, *38*, 2349–2356.
- (15) Mohan, S.; Pinto, B. M. Towards the elusive structure of kotalanol, a naturally occurring glucosidase inhibitor. *Nat. Prod. Rep.* **2010**, *27*, 481–488.
- (16) Tanaka, K. S. E.; Winters, G. C.; Batchelor, R. J.; Einstein, F. W. B.; Bennet, A. J. A new structural motif for the design of potent glucosidase inhibitors. *J. Am. Chem. Soc.* **2001**, *123*, 998–999.
- (17) Yuasa, H.; Izumi, M.; Hashimoto, H. Thiasugars: Potential Glycosidase Inhibitors. *Curr. Top. Med. Chem.* **2009**, *9*, 76–86.
- (18) Ogawa, S.; Yuasa, H. Hot Topic: The Medicinal Chemistry of Glycosidase Inhibitors. *Curr. Top. Med. Chem.* **2009**, *9*, 1–2.
- (19) Ogawa, S.; Kanto, M. Design and Synthesis of 5a-Carbaglycopyranosylamine Glycosidase Inhibitors. *Curr. Top. Med. Chem.* **2009**, *9*, 58–75.
- (20) Liu, Y.; Ma, L.; Chen, W.-H.; Wang, B.; Xu, Z.-L. Synthesis of xanthone derivatives with extended π -systems as α -glucosidase inhibitors: Insight into the probable binding mode. *Bioorg. Med. Chem.* **2007**, *15*, 2810–2814.
- (21) Liu, Y.; Zou, L.; Ma, L.; Chen, W.-H.; Wang, B.; Xu, Z.-L. Synthesis and pharmacological activities of xanthone derivatives as α -glucosidase inhibitors. *Bioorg. Med. Chem.* **2006**, *14*, 5683–5690.
- (22) Liu, Y.; Ke, Z. F.; Cui, J. F.; Chen, W. H.; Ma, L.; Wang, B. Synthesis, inhibitory activities, and QSAR study of xanthone derivatives as α -glucosidase inhibitors. *Bioorg. Med. Chem.* **2008**, *16*, 7185–7192.
- (23) Li, G. L.; He, J. Y.; Zhang, A. Q.; Wan, Y. Q.; Wang, B.; Chen, W. H. Toward potent α -glucosidase inhibitors based on xanthenes: A closer look into the structure-activity correlations. *Eur. J. Med. Chem.* **2011**, *46*, 4050–4055.
- (24) Kouam, S. F.; Khan, S. N.; Krohn, K.; Ngadjui, B. T.; Kapche, D.; Yapna, D. B.; Zareem, S.; Moustafa, A. M. Y.; Choudhary, M. I. α -glucosidase inhibitory anthranols, kenganthranols A-C, from the stem bark of *Harungana madagascariensis*. *J. Nat. Prod.* **2006**, *69*, 229–233.
- (25) Ngoupayo, J.; Nougoué, D. T.; Lenta, B. N.; Tabopda, T. K.; Khan, S. N.; Ngouela, S.; Shaiq, M. A.; Tsamo, E. Brevipsidone, a new depsidone and other α -glucosidase inhibitors from *Garcinia brevipedicellata* (Clusiaceae). *Nat. Prod. Commun.* **2007**, *2*, 1141–1144.
- (26) Seo, E. J.; Curtis-Long, M. J.; Lee, B. W.; Kim, H. Y.; Ryu, Y. B.; Jeong, T. S.; Lee, W. S.; Park, K. H. Xanthenes from *Cudrania tricuspidata* displaying potent α -glucosidase inhibition. *Bioorg. Med. Chem. Lett.* **2007**, *17*, 6421–6424.
- (27) Ngoupayo, J.; Tabopda, T. K.; Ali, M. S.; Tsamo, E. α -Glucosidase inhibitors from *Garcinia brevipedicellata* (Clusiaceae). *Chem. Pharm. Bull.* **2008**, *56*, 1466–1469.
- (28) Kram, K.; Khatmi, D.; Saihi, Y.; Ferkous, F.; Brahimi, M. Quantitative structure activity relationship for the computational prediction of α -glucosidase inhibitory. *Chemom. Intell. Lab. Syst.* **2009**, *97*, 118–126.
- (29) Srivastava, A. K.; Pandey, A.; Nath, A.; Jaiswal, M.; Pathak, V. K. Quantitative Structure Activity Relationship Studies On A Series Of Xanthone Derivatives As α -Glucosidase Inhibitors. *Oxid. Commun.* **2010**, *33*, 195–204.
- (30) Gao, L.; Zhou, Y.; Yan, H.; Huang, F.; Wen, R.; Li, G. Two New Xanthone Glucosidases From *Swertia Mussotii* Franch. *Heterocycles* **2011**, *83*, 1897–1902.
- (31) Su, Q. G.; Liu, Y.; Cai, Y. C.; Sun, Y. L.; Wang, B.; Xian, L. J. Anti-tumour effects of xanthone derivatives and the possible mechanisms of action. *Invest. New Drugs* **2011**, *29*, 1230–1240.
- (32) Ryu, H. W.; Cho, J. K.; Curtis-Long, M. J.; Yuk, H. J.; Kim, Y. S.; Jung, S.; Kim, Y. S.; Lee, B. W.; Park, K. H. α -Glucosidase inhibition and antihyperglycemic activity of prenylated xanthenes from *Garcinia mangostana*. *Phytochemistry* **2011**, *72*, 2148–2154.

- (33) Moorthy, N. S. H. N.; Ramos, M. J.; Fernandes, P. A. Topological, hydrophobicity, and other descriptors on alpha-glucosidase inhibition: a QSAR study on xanthone derivatives. *J. Enzyme Inhib. Med. Chem.* **2011**, *26*, 755–766.
- (34) Na, Y. Recent cancer drug development with xanthone structures. *J. Pharm. Pharmacol.* **2009**, *61*, 707–712.
- (35) Wan, L. S.; Min, Q. X.; Wang, Y. L.; Yue, Y. D.; Chen, J. C. Xanthone Glycoside Constituents of *Swertia kouitchensis* with alpha-Glucosidase Inhibitory Activity. *J. Nat. Prod.* **2013**, *76*, 1248–1253.
- (36) Lin, C. N.; Chung, M. I.; Liou, S. J.; Lee, T. H.; Wang, J. P. Synthesis and anti-inflammatory effects of xanthone derivatives. *J. Pharm. Pharmacol.* **1996**, *48*, 532–538.
- (37) Lin, C. N.; Hsieh, H. K.; Liou, S. J.; Ko, H. H.; Lin, H. C.; Chung, M. I.; Ko, F. N.; Liu, H. W.; Teng, C. M. Synthesis and antithrombotic effect of xanthone derivatives. *J. Pharm. Pharmacol.* **1996**, *48*, 887–890.
- (38) Saraiva, L.; Fresco, P.; Pinto, E.; Sousa, E.; Pinto, M.; Concalves, J. Synthesis and in vivo modulatory activity of protein kinase C of xanthone derivatives. *Bioorg. Med. Chem.* **2002**, *10*, 3219–3227.
- (39) Sanugul, K.; Akao, T.; Li, Y.; Kakiuchi, N.; Nakamura, N.; Hattori, M. Isolation of a Human Intestinal Bacterium That Transforms Mangiferin to Norathyriol and Inducibility of the Enzyme That Cleaves a C-Glucosyl Bond. *Biol. Pharm. Bull.* **2005**, *28*, 1672–1678.
- (40) Prashanth, D.; Amit, A.; Samiulla, D. S.; Asha, M. K.; Padmaja, R. α -Glucosidase inhibitory activity of *Mangifera indica* bark. *Fitoterapia* **2001**, *72*, 686–688.
- (41) Wang, Y. F.; Ma, L.; Li, Z.; Du, Z. Y.; Liu, Z.; Qin, J. K.; Wang, X. D.; Huang, Z. S.; Gu, L. Q.; Chen, A. S. C. Synergetic inhibition of metal ions and genistein on alpha-glucosidase. *FEBS Lett.* **2004**, *576*, 46–50.
- (42) Wang, Y. F.; Ma, L.; Pang, C.; Huang, M. J.; Huang, Z. S.; Gu, L. Q. Synergetic inhibition of genistein and D-glucose on alpha-glucosidase. *Bioorg. Med. Chem. Lett.* **2004**, *14*, 2947–2950.
- (43) Liu, M.; Zhang, W.; Wei, J.; Lin, X. Synthesis and alpha-glucosidase inhibitory mechanisms of bis(2,3-dibromo-4,5-dihydroxybenzyl) ether, a potential marine bromophenol alpha-glucosidase inhibitor. *Mar. Drugs* **2011**, *9*, 1554–1565.
- (44) Catanzano, F.; Graziano, G.; De Paola, B.; Barone, G.; D'Auria, S.; Rossi, M.; Nucci, R. Guanidine-induced denaturation of beta-glucosidase from *Sulfolobus solfataricus* expressed in *Escherichia coli*. *Biochemistry* **1998**, *37*, 14484–14490.
- (45) Liu, M.; Zhang, W.; Qiu, L.; Lin, X. Synthesis of butyl-isobutyl-phthalate and its interaction with alpha-glucosidase in vitro. *J. Biochem.* **2011**, *149*, 27–33.
- (46) Yang, J. T.; Wu, C. S.; Martinez, H. M. Calculation of protein conformation from circular dichroism. *Methods Enzymol.* **1986**, *130*, 208–269.
- (47) Park, H.; Hwang, K. Y.; Oh, K. H.; Kim, Y. H.; Lee, J. Y.; Kim, K. Discovery of novel alpha-glucosidase inhibitors based on the virtual screening with the homology-modeled protein structure. *Bioorg. Med. Chem.* **2008**, *16*, 284–292.
- (48) Park, H.; Hwang, K. Y.; Kim, Y. H.; Oh, K. H.; Lee, J. Y.; Kim, K. Discovery and biological evaluation of novel alpha-glucosidase inhibitors with in vivo antidiabetic effect. *Bioorg. Med. Chem. Lett.* **2008**, *18*, 3711–3715.
- (49) Watanabe, K.; Hata, Y.; Kizaki, H.; Katsube, Y.; Suzuki, Y. The refined crystal structure of *Bacillus cereus* oligo-1,6-glucosidase at 2.0 angstrom resolution: Structural characterization of proline-substitution sites for protein thermostabilization. *J. Mol. Biol.* **1997**, *269*, 142–153.
- (50) Thompson, J. D.; Higgins, D. G.; Gibson, T. J. CLUSTAL W: improving the sensitivity of progressive multiple sequence alignment through sequence weighting, position-specific gap penalties and weight matrix choice. *Nucleic Acids Res.* **1994**, *22*, 4673–4680.
- (51) Sali, A.; Blundell, T. L. Comparative protein modelling by satisfaction of spatial restraints. *J. Mol. Biol.* **1993**, *234*, 779–815.
- (52) Sippl, M. J. Recognition of errors in three-dimensional structures of proteins. *Proteins* **1993**, *17*, 355–362.
- (53) Morris, G. M.; Huey, R.; Lindstrom, W.; Sanner, M. F.; Belew, R. K.; Goodsell, D. S.; Olson, A. J. AutoDock4 and AutoDockTools4: Automated Docking with Selective Receptor Flexibility. *J. Comput. Chem.* **2009**, *30*, 2785–2791.
- (54) Baker, D.; Sali, A. Protein structure prediction and structural genomics. *Science* **2001**, *294*, 93–96.
- (55) Ferreira, S. B.; Sodero, A. C. R.; Cardoso, M. F. C.; Lima, E. S.; Kaiser, C. R.; Silva, F. P.; Ferreira, V. F. Synthesis, Biological Activity, and Molecular Modeling Studies of 1H-1,2,3-Triazole Derivatives of Carbohydrates as alpha-Glucosidases Inhibitors. *J. Med. Chem.* **2010**, *53*, 2364–2375.
- (56) Adisakwattana, S.; Charoenlertkul, P.; Yibchok-anun, S. alpha-Glucosidase inhibitory activity of cyanidin-3-galactoside and synergistic effect with acarbose. *J. Enzyme Inhib. Med. Chem.* **2009**, *24*, 65–69.